Sustainable Production through Advanced Manufacturing, Intelligent Automation and Work Integrated Learning, J. Andersson et al. (Eds.)

doi:10.3233/ATDE240156

Influence of Processes and Process Variables for WAAM - Geometry of Deposited Bead

Peigang Li [a,1] , Yazan Al-Hallis [a,2], Rani Al-Chafey [a,3]
[a] *Engineering Science Department, Högskolan Väst*

ORCiD ID: Peigang Li https://orcid.org/0000-0003-4548-7302

Abstract. Wire Arc Additive Manufacturing (WAAM) is developing rapidly in recent years due to its advantages, such as higher productivity, lower cost, acceptable quality, and the availability of advanced welding processes. Cold Metal Transfer (CMT), as the most well-known Gas Metal Arc Welding (GMAW) process, is widely used in WAAM. The uniqueness of CMT lies in minimizing the heat input of the process. However, there is a drawback to the lower heat input, impacting the quality of the geometry of the welding bead, sharp transitions at the weld toe, inclusions, etc., particularly for higher alloyed steel, e.g., tool steel. In this study, two processes were employed: CMT and Pulse Multi Control (PMC). Two types of shielding gases were used, namely 2% CO2 + 98% Ar and 20% CO2 + 80% Ar. Two levels of wire feed speed were selected: high and low levels. A full-fraction factorial experimental matrix was created, and bead-on-plate samples were produced with different GMAW processes, i.e., CMT and PMC. The geometry of the bead-on-plate, including penetration, bead width and height, and toe angle, was evaluated and analyzed. A correlation between the process factors (shielding gas, type of process, and wire feed speed) and the geometry of the bead was analyzed and determined. A protocol is proposed based on the study results for the selection of WAAM processes.

Keywords. WAAM, Process parameter, GMAW, Geometry, Weld toe angle

1. Introduction

Wire Arc Additive Manufacturing (WAAM) stands out as a promising technology within the realm of Additive Manufacturing (AM), facilitating the construction of predefined parts geometries. WAAM has gained prominence for its role in mass production as a form of direct energy deposition AM. In recent years, it has experienced substantial growth, owing to its numerous advantages compared to other methods, including higher productivity, the capacity for manufacturing large components, widespread availability of the WAAM process, lower costs, minimal material wastage, and the simplicity of feedstock, among others [1, 2].

[1] Corresponding Author: Peigang Li, Engineering Science Department, Högskolan Väst, Peigang.li@hv.se Tel: 0520 22 33 95.

WAAM is increasingly recognized as a viable alternative to traditional manufacturing methods such as forging and casting, especially for complex designs. Its versatility extends to a wide range of materials, including high-strength steel, aluminium, stainless steel, nickel alloy, and titanium. This broad material applicability positions WAAM as a valuable technology in various industries, encompassing general manufacturing, shipping, automotive and vehicle production, as well as applications in the space and aeronautics sectors [3, 4].

Gas Metal Arc Welding-based Additive Manufacturing (GMAW-AM) is a specific approach that utilizes low-cost equipment, taking advantage of the readily available GMAW welding equipment in the existing market. This equipment demonstrates the capability and flexibility required for fabricating components with large and moderately complex geometries. Advanced GMAW welding processes, such as Cold Metal Transfer (CMT) and controlled pulse welding, have garnered significant attention from researchers and industries, spurring exploration within the realm of GMAW-based Wire Arc Additive Manufacturing (WAAM) [5].

Cold Metal Transfer (CMT) is an innovative GMAW technique distinguished by its unique feature of pulling the filler metal wire backward after a short circuit. This retraction of the wire facilitates droplet detachment during the short circuit, resulting in minimized energy input and reduced spattering, while maintaining a stable arc. The low heat input characteristic of CMT is particularly advantageous for minimizing distortions and achieving optimal penetration, making it an ideal choice for welding thin sheets. These features collectively make CMT well-suited for applications in WAAM [6, 7].

Despite the utilization of advanced processes, WAAM encounters challenges in ensuring the quality of its products. These challenges encompass issues such as surface formation, dimension tolerance, mechanical properties, hardness, multi-thermal impact, metallurgy, and microstructure properties. Notably, these challenges, particularly those related to surface quality, may hinder the widespread application of WAAM in manufacturing high-quality components [8, 9]. Additionally, the arc characteristics of WAAM and its extended process cycle time present challenges for implementing an automatic monitoring system to detect defects and non-conformances [10].

Therefore, investigating the correlation between geometry and WAAM variables is crucial. Huang et al. [11] employed advanced 3D scanning to characterize the surface geometry of side walls built by CMT-WAAM. The study also conducted mechanical property analyses using tensile tests. However, the study only varied wire feed rate and travel speed. Karmuhilan et al. [12] utilized an advanced approach, the artificial neural network (ANN) model, to analyze the correlation between geometry and process variables, including two types of shielding gases and one type of metal transfer mode (pulse spray). Novelino et al. [13] focused on investigating the correlation between CMT deposition parameters and wall geometry. In the study, not only was the side wall geometry characterized, but the bead-on-plate weldment geometry was also evaluated. This can be considered an indicator reflecting the built geometry in WAAM.

As a type of GMAW process, it is well known that shielding gas plays a crucial role in influencing bead formation, especially in CMT [14-16]. As mentioned earlier, numerous studies have investigated the impact of factors such as wire feed speed, GMAW process type, travel speed, etc., on bead geometry individually. Unfortunately, there is a scarcity of research encompassing all three aspects in a single study wire feed rate, GMAW process (CMT or Pulse), and shielding gas.

This study comprehensively considers all three aspects, employing both CMT and Pulse Multi Control (PMC) as different GMAW processes. Two levels of wire feed speed

and two types of shielding gas, each with different levels of active gas content, are investigated, with a specific focus on evaluating the characteristics of the deposited bead-on-plate. The aim is to establish a protocol and guideline for WAAM concerning the selection of process type, shielding gas type, and wire feed speed.

2. Experimental

2.1 Deposition of bead-on-plate samples

Deposited samples were fabricated using a robotized WAAM system, featuring an ABB IRB 2600 robot and a welding machine Fronius TPS 500i with CMT and PMC processes. A full factorial fractional design was employed with three main welding variables: process, gas composition, and wire feed speed. This design produced eight bead-on-plate welding beads, each approximately 200mm in length, as schematically shown in **Figure 1**. The electrical signals, including current and voltage, were recorded using the Fronius power source.

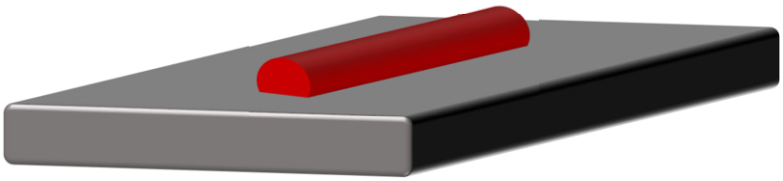

Figure 1 Schematic figure of bead-on-plate sample.

Tool steel with a consumable diameter of 1.2 mm was utilized, and its chemical composition is detailed in **Table 1**. Two types of shielding gases, namely 2% CO2 + 98% Ar and 20% CO2 + 80% Ar, were employed. Two levels of wire feed speed were chosen based on pre-tests aimed at optimizing arc stability. The travel speed (TS) remained constant at TS=6mm/s, a carefully determined value derived from a pre-study to ensure the avoidance of irregular welding bead formation. The deposition experimental matrix was generated using a full factorial fractional design, as illustrated in **Table 2**.

Table 1 Chemical composition of deposition consumable.

C	Si	Mn	Cr	Mo	V	Fe
0.6	0.35	0.8	4.5	0.5	0.2	Bal.

Table 2 Experimental matrix with deposition parameters.

Run Nr.	Process	Gas composition	WFS (m/min)	Current (A)	Voltage(V)
1	PMC	2%CO2+ 98%Ar	10	245	25.7
2	PMC	2%CO2+ 98%Ar	3	95	18.1
3	PMC	20%CO2+ 80%Ar	3	92	19.0
4	PMC	20%CO2+ 80%Ar	10	235	25.4
5	CMT	2%CO2+ 98%Ar	10	269	19.4
6	CMT	2%CO2+ 98%Ar	3	99	13.7
7	CMT	20%CO2+ 80%Ar	3	81	14.9
8	CMT	20%CO2+ 80%Ar	10	259	19.8

2.2. Metallographic test

Three metallographic samples were cut from a single deposited bead using a Buehler Abrasimet 2 abrasive hand saw, as indicated by A, B, and C in **Figure 2**. The samples were labelled based on the deposition direction, and specifically, three samples were positioned at a distance of 20mm away from the start/stop of the bead to mitigate the influence of an unstable arc.

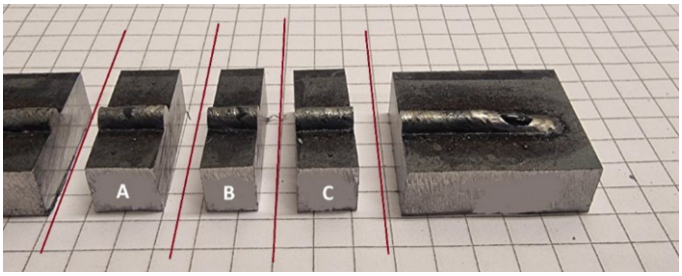

Figure 2: Example showing location of cut metallographic sample on one deposition bead.

A total of 24 samples were mounted using Buehler Epomet G molding compound with the Buehler Simplimet 2000 machine. These samples were prepared using the Buehler Automet 300, involving grinding and polishing down to 3µm. To enhance the visibility of penetration, Nital 5% was employed as an etchant for etching the samples.

Examinations were conducted using a Zeiss Axio Imager M2M microscope under 5x magnification. The geometry of the bead, which includes penetration, bead width, bead height (reinforcement), and weld toe angle, was measured using the Zeiss Zencore 2.7 software, as illustrated in **Figure 3**.

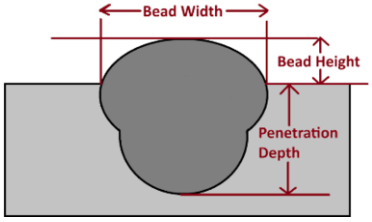

(a) Schematic illustration of measurement of bead width, bead height, and penetration

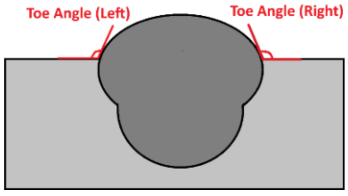

(b) Schematic illustration of measurement of toe angles

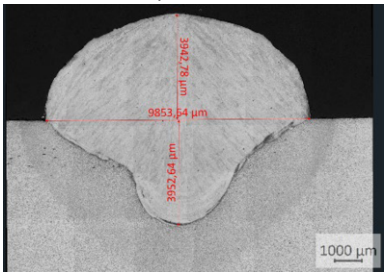

(c) Example of measurement of bead width, bead height, and penetration

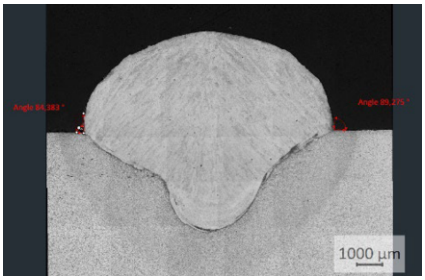

(d) Example of measurement of toe angles

Figure 3: Illustration of methodology measuring penetration, bead width, bead height and toe angles.

3. Results

Arc power was recorded and calculated using current and voltage data, as depicted in **Figure 4**. Two calculation methods were employed: one utilized the measured average current and voltage values with the equation (1), referred to as 'Average Power.' The second method involved using instantaneous values of current and voltage (at 10Hz) and the algorithm calculated the average power with the equation (2), referred to as 'InstPower' (instantaneous power). It's important to note that the two calculation methods showed negligible differences for both welding processes (CMT and PMC), as indicated in the value table in **Figure 4**.

$$Power = U * I \tag{1}$$

$$Power = (\sum_{i=1}^{n} U_i * I_i)/n \tag{2}$$

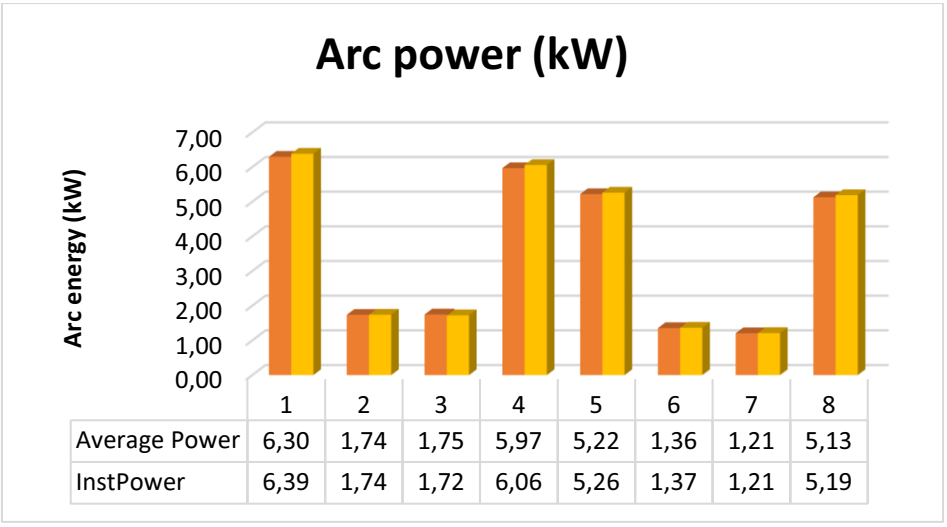

	1	2	3	4	5	6	7	8
Average Power	6,30	1,74	1,75	5,97	5,22	1,36	1,21	5,13
InstPower	6,39	1,74	1,72	6,06	5,26	1,37	1,21	5,19

Figure 4 The arc power of welding with different parameters.

The analysis of the deposited bead geometry included measurements of penetration, bead width, bead height, and toe angle. Three cross-sections were prepared and measured, and the results, along with standard deviations, are presented in **Table 3**. It is worth noting that the standard deviation did not significantly influence the results compared to the variations observed between different beads and deposition conditions, as illustrated in **Figure 5**. The toe angle measurements are detailed in **Table 4**, with both the average value and standard deviation depicted in **Figure 6**.

Table 3 Measured value and standard deviation of penetration, bead width and bead height.

Sample Nr.	Penetration (µm)	STEDV	Bead width (µm)	STEDV	Bead Height (µm)	STEDV
1	4034,68	196,23	9968,93	196,23	3920,28	311,46
2	1208,29	54,65	5797,59	54,65	2207,15	478,76
3	1304,82	198,85	5189,59	198,85	2038,07	143,34
4	3679,02	113,04	9087,41	113,04	4053,90	70,71
5	3109,45	85,57	7648,78	85,57	4530,21	264,72
6	540,90	62,65	3482,75	62,65	2935,03	259,06
7	609,90	60,93	3238,51	60,93	2173,15	99,57
8	2698,35	86,53	7698,16	86,53	4033,67	105,46

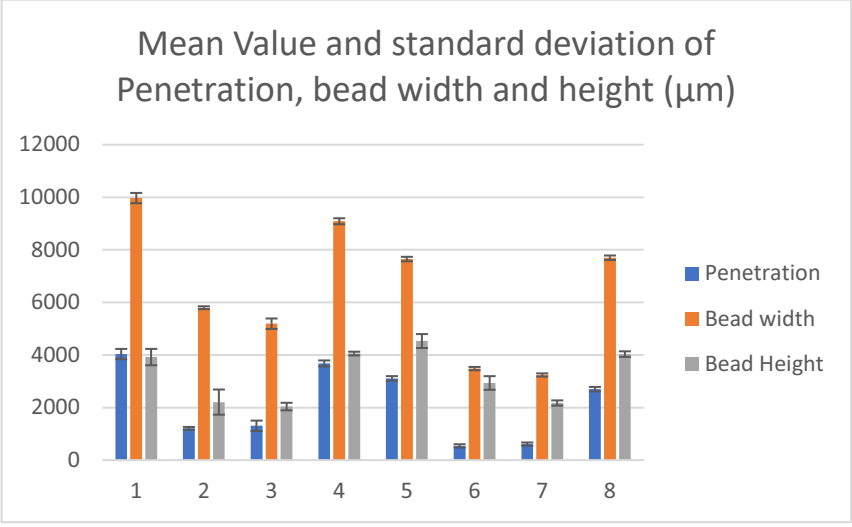

Figure 5 Standard deviation of penetration, bead width and height.

Table 4 Measurement of weld toe.

Sample Nr.	1	2	3	4	5	6	7	8
Toe angle (°)	92,94	110,64	114,56	96,08	82,12	81,72	86,51	84,33
STDEV	11,75	19,16	16,53	10,87	12,48	15,15	6,23	10,43

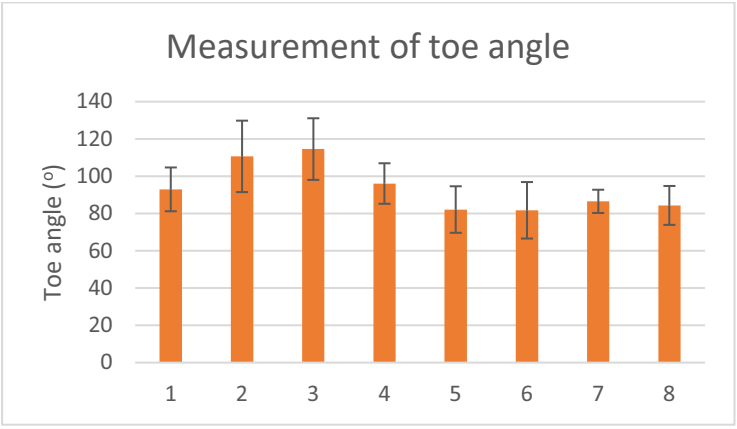

Figure 6. Toe angle of deposited bead.

4. Discussion

MODDE was employed for statistical analysis of the coefficients of different parameters and interactions. The summary of the coefficients is presented in **Figure 7**.

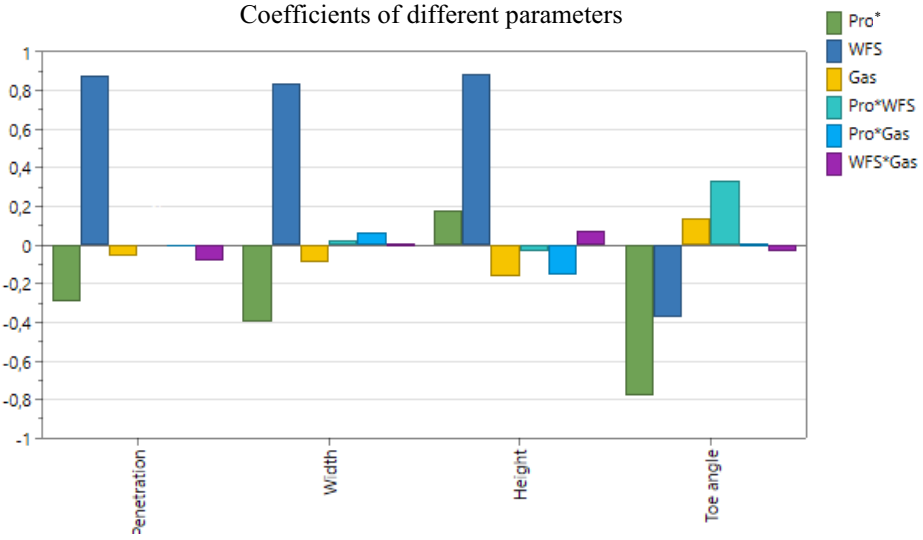

*: 'Pro' refers to welding process

Figure 7 Summary of coefficients of deposition factors and its interactions.

According to **Figure 7**, the wire feed speed (WFS) exhibits the most significant and positive impact on geometry factors specifically, penetration, width, and height. WFS also demonstrates a secondary but significant influence on the weld toe angle. In essence, a higher WFS corresponds to increased penetration and a 'larger' bead (higher width and height simultaneously), as illustrated in **Figure 8**. This is attributed to the elevated current and the amount of wire deposited onto the workpiece essentially, the volume of deposition material. Conversely, an increased WFS results in a smaller toe angle, as

depicted in **Figure 9**. A reduced toe angle can sometimes lead to defects like lack of fusion or inclusions, especially with improper WAAM process factors, such as an inappropriate overlap ratio. Additionally, it may constrain the application of higher travel speed.

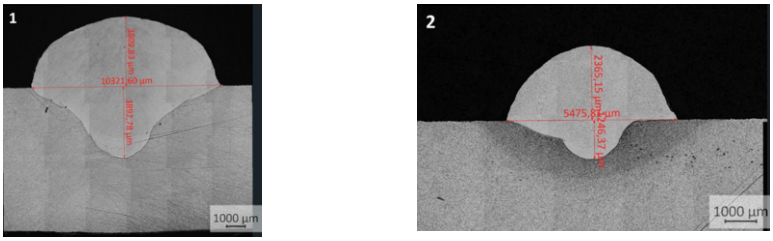

WFS=10m/min WFS=3m/min

Figure 8 Picture shows a deeper penetration, wider and higher deposition bead with higher WFS.

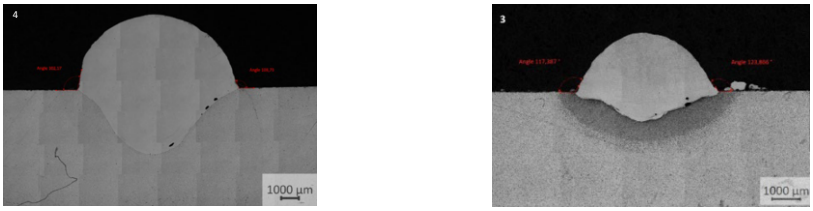

WFS 10m/min WFS 3m/min

Figure 9 A decreased toe angle with increased WFS.

Concerning the process type, **Figure 10** indicates that the application of CMT has a secondary, significant, and negative impact on penetration, width, and toe angle of the bead. This is particularly noticeable in the case of toe angle, where a significantly smaller toe angle is observed with CMT compared PMC. This smaller toe angle can potentially lead to quality issues, especially when there is an overlap between beads. Moreover, the application of CMT has a positive impact on the height of the deposited bead. In summary, CMT tends to produce a narrow and high bead, in contrast to PMC, which tends to result in a wider and lower bead with a larger toe angle, as illustrated in **Figure 10**.

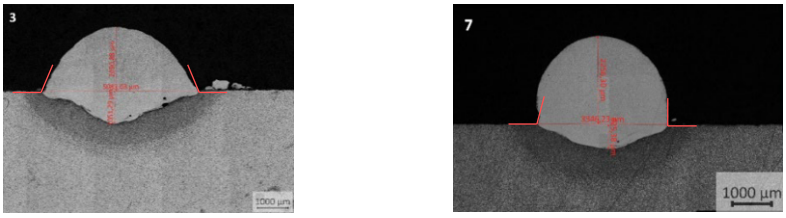

PMC CMT

Figure 10 Decreased penetration, width of bead and increased height of CMT deposition compared with PMC.

Finally, regarding the shielding gas, its impact appears to be less distinct for penetration, bead width, and bead height. One possible explanation could be the controlled current and voltage by the power source, primarily determined by the set wire feed speed, as shown in **Table 2**. However, the influence of the shielding gas on toe angle is notably more significant than that of all the other three geometry factors. A higher content of carbon dioxide tends to result in a higher toe angle, as illustrated in **Figure 11** and **Figure 6**. As discussed earlier, a higher toe angle can contribute to minimizing the risk of imperfections in Wire Arc Additive Manufacturing (WAAM).

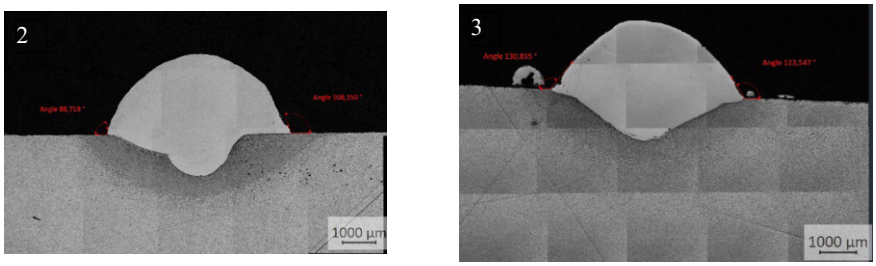

Figure 11 Influence of gas on weld toe angle.

In the context of WAAM, process requirements may vary based on the parts design whether it involves thin-wall construction or a bulky build. According to the results of this study, a qualitative protocol can be proposed. CMT with a lower carbon dioxide shielding gas is preferable for thin-wall construction. The wire feed speed can be determined based on the width of the wall. On the other hand, PMC is recommended for a bulky build with higher carbon dioxide shielding gas. Careful consideration of the wire feed speed is essential to optimize weld toe formation and reduce the risk of imperfections.

5. Conclusions

In the investigation of three deposition factors process type, wire feed speed, and shielding gas composition through the geometry analysis of 24 deposited beads, the following key findings were observed:

- Wire feed speed: Demonstrated the most significant influence on the geometry of the deposited bead, particularly on penetration, bead width, and height. This can be attributed to its substantial impact on the volume of deposited material.
- Process type: Exhibited a secondary but significant influence on all geometry factors, including penetration, bead width, height, and toe angle. Notably, for toe angle, process type had a more substantial impact than wire feed speed. This aspect should be carefully considered when selecting a process for Wire Arc Additive Manufacturing (WAAM).
- Shielding gas: Showed negligible influence toe angles. More active gas components tended to result in larger toe angles. This factor should be taken into account for geometry improvement in WAAM when the volume of deposition material has been determined.

- Considering different applications and designs for WAAM-built parts, the selection of processes and parameters should be done meticulously. Based on the results of this study, a qualitative protocol is recommended. For thin-wall construction, it is suggested to use the Cold Metal Transfer (CMT) process with a lower level of carbon dioxide and optimize wire feed speed based on wall thickness. For bulky builds, a pulsed arc GMAW process (e.g. Pulse Multi Control (PMC)), with a higher level of carbon dioxide in shielding gas and optimized wire feed speed, is recommended.

Acknowledgement

Special acknowledgment is extended to the DEDICATE project from KAM-PT, Högskolan Väst, and the KK Foundation. Gratitude is expressed for the invaluable assistance provided by Mr. Björn Särnerblom in conducting metallographic tests and Mr. Hettiachchi Mudiyanselage Madushka Malan Jayawickrama for his support in the laboratory.

References

[1] Kabliman, E., et al., Chapter Twelve - Wire arc additive manufacturing of light metals: From experimental investigation to numerical process simulation and microstructural modeling, in Quality Analysis of Additively Manufactured Metals, J. Kadkhodapour, S. Schmauder, and F. Sajadi, Editors. 2023, Elsevier. p. 487-546.

[2] Kawalkar, R., H.K. Dubey, and S. Lokhande, Chapter 10 - Wire arc additive manufacturing: A comprehensive review on methodologies and processes to overcome challenges with metallic alloys, in Innovative Processes and Materials in Additive Manufacturing, S. Singh, C. Prakash, and S. Ramakrishna, Editors. 2023, Woodhead Publishing. p. 191-258.

[3] Chalasani, D. and M. Mohammadi, Chapter Fifteen - Prospects of additively manufactured nickel aluminum bronzes for marine applications, in Quality Analysis of Additively Manufactured Metals, J. Kadkhodapour, S. Schmauder, and F. Sajadi, Editors. 2023, Elsevier. p. 627-687.

[4] Jhavar, S., Chapter 9 - Wire arc additive manufacturing: approaches and future prospects, in Additive Manufacturing, M. Manjaiah, et al., Editors. 2021, Woodhead Publishing. p. 183-208.

[5] Pattanayak, S. and S.K. Sahoo, Gas metal arc welding based additive manufacturing—a review. CIRP Journal of Manufacturing Science and Technology, 2021. **33**: p. 398-442.

[6] Selvi, S., A. Vishvaksenan, and E. Rajasekar, Cold metal transfer (CMT) technology - An overview. Defence Technology, 2018. **14**(1): p. 28-44.

[7] Tankova, T., et al., Characterization of robotized CMT-WAAM carbon steel. Journal of Constructional Steel Research, 2022. **199**: p. 107624.

[8] Kumar Sinha, A., S. Pramanik, and K.P. Yagati, Research progress in arc based additive manufacturing of aluminium alloys – A review. Measurement, 2022. **200**.

[9] Zahidin, M.R., et al., Research challenges, quality control and monitoring strategy for Wire Arc Additive Manufacturing. Journal of Materials Research and Technology, 2023. **24**: p. 2769-2794.

[10] Xia, C., et al., A review on wire arc additive manufacturing: Monitoring, control and a framework of automated system. Journal of Manufacturing Systems, 2020. **57**: p. 31-45.

[11] Huang, Y., L. Yang, and Q. Xin, Novel geometrical model and design mechanical parameters for CMT-WAAM stainless steel. Journal of Constructional Steel Research, 2023. **210**.

[12] Karmuhilan, M. and A.k. sood, Intelligent process model for bead geometry prediction in WAAM. Materials Today: Proceedings, 2018. **5**(11): p. 24005-24013.

[13] Novelino, A.L.B., G.C. Carvalho, and M. Ziberov, Influence of WAAM-CMT deposition parameters on wall geometry. Advances in Industrial and Manufacturing Engineering, 2022. **5**: p. 100105.

[14] Norrish, J., 7 - Gas metal arc welding, in Advanced Welding Processes, J. Norrish, Editor. 2006, Woodhead Publishing. p. 100-135.

[15] da Silva, L.J., et al., Effect of O2 content in argon-based shielding gas on arc wandering in WAAM of aluminum thin walls. CIRP Journal of Manufacturing Science and Technology, 2021. **32**: p. 338-345.

[16] Zhao, W., et al., Deepening the understanding of arc characteristics and metal properties in GMAW-based WAAM with wire retraction via a multi-physics model. Journal of Manufacturing Processes, 2023. **97**: p. 260-274.